A Lightweight Secure Image Super Resolution Using Network Coding

Quoc-Tuan Vien[1][a], Tuan T. Nguyen[2][b] and Huan X. Nguyen[1][c]

[1]*Faculty of Science and Technology, Middlesex University, The Burroughs, London NW4 4BT, United Kingdom.*

[2]*School of Computing, Buckingham University, Hunter St, Buckingham MK18 1EG, United Kingdom.*

{*Q.Vien, H.Nguyen*}*@mdx.ac.uk, Tuan.Nguyen@buckingham.ac.uk*

Abstract: Images play an important part in our daily life. They convey our personal stories and maintain meaningful objects, events, emotions etc. People, therefore, mostly use images as visual information for their communication with each other. Data size and privacy are, however, two of important aspects whilst transmitting data through network like internet, i.e. the time prolongs when the amount of data are increased and the risk of exposing private data when being captured and accessed by irrelevant people. In this paper, we introduce a unified framework, namely Deep-NC, to address these problems seamlessly. Our method contains three important components: the first component, adopted from Random Linear Network Coding (RLNC), to protect the sharing of private image from the eavesdropper; the second component to remove noise causing to image data due to transmission over wireless media; and the third component, utilising Image Super-Resolution (ISR) with Deep Learning (DL), to recover high-resolution images from low-resolution ones due to image sizes reduced. This is a general framework in which each component can be enhanced by sophisticated methods. Simulation results show that an outperformance of up to 32 dB, in terms of Peak Signal-to-Noise Ratio (PSNR), can be obtained when the eavesdropper does not have any knowledge of parameters and the reference image used in the mixing schemes. Various impacts of the method are deeply evaluated to show its effectiveness in securing transmitted images. Furthermore, the original image is shown to be able to downscale to a much lower resolution for saving significantly the transmission bandwidth with negligible performance loss.

1 INTRODUCTION

Deep Learning (DL) has recently received increasing attention and achieves impressive results across a spectrum of domains such as medicine, automation, transportation, security, and so forth. It is a specific sub-field of machine learning that uses neural network with multiple layers. Each layer represents a deeper level of knowledge. DL learns representations from data through successive layers to increase meaningful representations.

The reasons for the success of DL can be attributed to two folds: first, the feature learning (Goodfellow et al., 2016) capacity of its hierarchical architecture allows for automatically extracting meaningful features from data, in which lower layers identify basic features, and deeper layers synthesize higher-level features in terms of learned lower-level ones; second, the development of high-performance computers with Graphic Processing Units and Tensor Processing Units enable to perform a large number of operations in reduced CPU times. Moreover, with the increasing digitisation transformation, the applicability of DL is more pronounced as the bigger data become, the larger DL architecture is expected, and vice versa, to capture underlying patterns better.

Research has proven that DL is one of effective techniques for Super Resolution (SR) tasks with the development of multiple DL based architectures. SR is the process of recovering a High-Resolution (HR) image from a given Low-Resolution (LR) image (Kim et al., 2016). An LR image is an image which has a reduced dimension or contains noise or blurring regions. The relationship between an HR image and an LR image can be represented by a function which allows us to invert the LR image back to the HR image. If the invert function is known, the HR image can be easily reconstructed from the LR image. In reality, this is, however, not the case. The core problem of the SR is to create a mapping between the LR and HR images. Although there are a va-

---

[a] https://orcid.org/0000-0001-5490-904X

[b] https://orcid.org/0000-0003-0055-8218

[c] https://orcid.org/0000-0002-4105-2558

riety of approaches, they can be grouped into four main architecture types (Wang et al., 2020) including: i) Pre-upsampling with bi-cubic (Keys, 1981) and bi-linear interpolation (Smith, 1981); ii) Post-upsampling at the last learnable layer; iii) Progressive Upsampling with Laplacian pyramid SR framework (LapSRN) (Lai et al., 2017); and iv) Iterative Up and Down Sampling SR with back-projection (Irani and Peleg, 1991), DBPN (Haris et al., 2018) and SRFBN (Li et al., 2019b).

Nowadays, data transfer is a crucial part of our daily life and in multiple areas. Multiple techniques have been introduced to transmit data efficiently. Network coding (NC) is one of them. Its concept (Ahlswede et al., 2000) has been well exploited in a vast number of research work from networking and communications perspective aiming to increase the system throughput by allowing the intermediate nodes to perform encoding the incoming data rather than operating simply as store-and-forward switches. Specifically, an algebraic approach of NC, namely random linear NC (RLNC), was developed in (Koetter and Medard, 2003) where the intermediate nodes can perform random linear operations on the incoming data packets from different transmission source nodes. The sink nodes with a sufficient number of mixed data packets along with all RLNC coefficients can recover the data of all source nodes.

Digital images contain quite a lot of essential information and are widely used to communicate between people over internet. Several issues encounter during transmission such as data privacy and reducing amount of data transferred to lessen the transmission time. Various methods are developed to protect them such as stenography, encryption, and watermarking. Stenography is a method to hide data inside an image. In the encryption approach, one image is converted into an encrypted image by using the secret key. The core idea of the encrypted image is to turn understandable data into incomprehensible data which are hard to realise. On the other hand, watermarking techniques are to embed the signature into an image to visualise or hide the ownership of the image.

In general, steganography and encryption are different but they serve one main purpose, protecting necessary data from irrelevant people. Encryption is more flexible and secure (Xie et al., 2019; Guerrini et al., 2020; Peng et al., 2020). Human, however, is always curious and tries to see what messages when they receive encrypted information. In such cases, steganography is a better option because the hidden message can be embedded so that the change of image will not be noticed and does not draw attention (Bender et al., 1996; Franz et al., 1996; Chen and Lin, 2006). This technique nevertheless requires the hidden message to have a smaller size than the cover image's, meaning that hiding an image into another image is not easily achievable.

Different from multiple works solely focusing on data security, or interested in data compression, our work integrates both techniques together to gain a better information protection. This aim is to develop a simple yet efficient method to conceal and reduce the file size whilst transmitting image data through network. When the data is received, it can be easily recovered at the other end. Inspired by the NC concept, a secure Image SR (ISR) using DL and NC, namely Deep-NC, is proposed and demonstrated in the scenario for an image communication between Alice and Bob.

In the proposed Deep-NC, the downscaled image, i.e. LR version of the original image, is incorporated with the reference image by RLNC encoding prior to transmitting to Bob. Over noisy channel, the received image at Bob is denoised, followed by RLNC decoding using the shared reference image and VDSR for recovering the original image of high resolution. The performance of the proposed Deep-NC is evaluated in terms of Peak Signal-to-Noise Ratio (PSNR) taking into account additive white Gaussian noise model. The impacts of RLNC, shared image dataset, noise and scaling factor on the performance are assessed through simulation to validate the effectiveness of the proposed scheme. Simulation results show that Bob achieves a far better performance than Eve with the employment of Deep-NC, especially when the Eve has no knowledge of the reference image shared between Alice and Bob. Additionally, both VDSR and bicubic interpolation are shown to provide a better performance at Bob compared to Eve. Furthermore, the proposed Deep-NC allows the image to be downscaled to a much lower resolution to save the transmission bandwidth, while still maintaining a significantly higher performance than Eve.

2 SYSTEM MODEL

A typical secure image communication model is considered where Alice ($\mathcal{A}$) wants to send a private image to Bob ($\mathcal{B}$) in the existence of Eve ($\mathcal{E}$) trying to eavesdrop the image.

Let I_A denote the original image of size $M \times N$ that Alice wants to send. Considering typical colour images with three channels, i.e. red, green and blue, I_A can be defined as an $M \times N \times 3$ array, i.e.

$$I_A : f(x_A, y_A) \to \mathbb{R}^3, \qquad (1)$$

where $f(x_A, y_A) \in \mathbb{R}$ is the intensity of the image pixel at point (x_A, y_A). Over the transmission media, the noise is inevitable, which causes image degradation. Generally, Gaussian noise model has been regarded as the best fit in representing the additive noise in the undesired signal at the receiver in most of communication systems due to its simplicity with dominant central limit theorem.

Considering additive noise model, the image received at node X, $X \in \{\mathcal{B}, \mathcal{E}\}$, is given by

$$I_X = I_A + N_X, \tag{2}$$

where N_X, $X \in \{B, E\}$, is additive white Gaussian noise (AWGN) at X having mean μ_X and variance σ_X^2.

In order to denoise an image with AWGN, a deep neural network can be employed, e.g. a pretrained DnCNN network (Zhang et al., 2017).

3 PROPOSED SECURE ISR

Our proposed approach is shown in the flowchart, Fig. 1, which consists of the following main steps:[1]

3.1 Downscaling at Alice

In order to save the transmission bandwidth, a LR version of the original image is firstly generated using bicubic interpolation. The bicubic filter is employed for downscaling due to its low computational complexity, while preserving image details with smooth interpolated surface.[2]

After downscaling the original image, i.e. I_A, from Alice, we have a LR image I'_A having size $\lceil M/\delta \rceil \times \lceil N/\delta \rceil \times 3$ where δ denotes the scaling factor and $\lceil x \rceil$ denotes the ceiling function of x.

3.2 RLNC Encoding at Alice

Following the concept of RLNC (Koetter and Medard, 2003), in the proposed scheme, the downscaled image at Alice is linearly mixed with a reference image using random scalar coefficients, a.k.a. RLNC coefficients. The reference image is acquired from an image datastore which is assumed to be shared between

users as a common image dataset.[3]

In order to mix two images, the shared image is first downscaled to the same size of the original LR image. Let I_S and I'_S denote the HR and LR shared image, respectively. I'_S should have the same size of I'_A, i.e. an $\lceil M/\delta \rceil \times \lceil N/\delta \rceil \times 3$ array.

The mixing of the original image and the shared image can be realised as follows:

$$I_T = \alpha_A I'_A + \alpha_S I'_S, \tag{3}$$

where I_T denotes the transmitted image at Alice, α_A and α_S are RLNC coefficients having $\alpha_A > 0$, $\alpha_S \geq 0$ and $\alpha_A + \alpha_S = 1$. Here, α_A and α_S represent the fractions of original image and shared image, respectively, in the mixed image.

Remark 1 (image decodability-security tradeoff)

A higher α_A results in a better performance at Bob with an enhanced image decodability, while a higher α_S helps secure the original image from Eve. In fact, a higher α_A means more information of the original image in the mixed image, and thus Bob can recover the desired image with higher decodability. However, Eve also overhears the same amount of information to be able to extract the original image, which means more information at the same time is leaked to Eve. On the other hand, a higher α_S, i.e. a lower α_A, causes degradation of the image decodability at Bob, but it helps improve the secrecy of the image communications due to less information of the original image in the image mixture. Therefore, it is crucial to find α_A (or α_S) to balance the tradeoff between the image decodability and security.

3.3 Denoise at Bob and Eve

Over the noisy channel, the image transmitted from Alice is deteriorated caused by Gaussian noise. It is assumed that Eve experiences the same noisy environment as Bob.

The images received at $\mathcal{B}$ and $\mathcal{E}$ over Gaussian noise model can be obtained as in (2), i.e.

$$I_X = I_T + N_X, \tag{4}$$

where $X \in \{B, E\}$ and I_T is the transmitted image at Alice given by (3). Both $\mathcal{B}$ and $\mathcal{E}$ then remove the Gaussian noise using the same pretrained DnCNN network.

Let us denote the denoised images at $\mathcal{B}$ and $\mathcal{E}$ after filtering by $\tilde{I}_B$ and $\tilde{I}_E$, respectively.

---

[1]Note that common blocks at Bob and Eve to represent the same steps are combined in the following discussion.

[2]There exist different downscaling methods, e.g. Box sampling, Nearest-neighbour interpolation, Lanczos Filtering (Duchon, 1979), or CNN based downscaling like (Li et al., 2019a); however, we do not need a sophisticated downscaling method in this work.

[3]Notice that only RLNC coeffients and the index of the reference image are shared between Alice and Bob prior to transmission as private keys in key-agreement protocols.
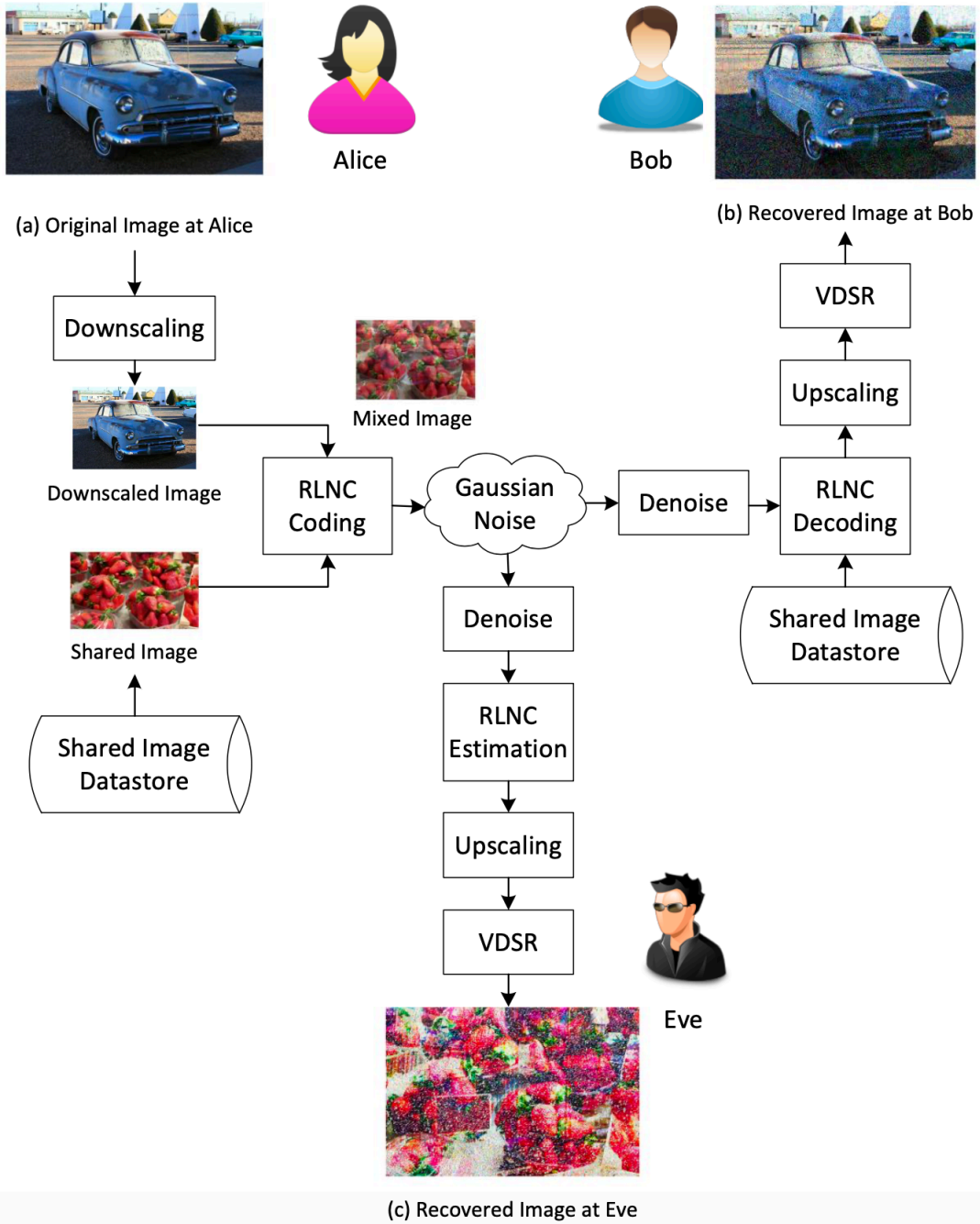
(a) Original Image at Alice

(b) Recovered Image at Bob

Alice

Bob

Downscaling

Downscaled Image

Mixed Image

Shared Image

Shared Image
Datastore

RLNC
Coding

Gaussian
Noise

Denoise

Denoise

RLNC
Estimation

Upscaling

VDSR

VDSR

Upscaling

RLNC
Decoding

Shared Image
Datastore

Eve

(c) Recovered Image at Eve

Figure 1: Proposed Deep-NC for secure ISR

3.4 RLNC Decoding at Bob

Given the index of the reference image in the shared image datastore and RLNC coefficients, i.e. α_A or α_S, Bob can recover the image transmitted from Alice as

$$\hat{I}'_B = \frac{1}{\alpha_A} \left(\tilde{I}_B - \alpha_S I'_S \right), \tag{5}$$

where I'_S is the LR version of the shared image and $\hat{I}'_B$ is the decoded image at $\mathcal{B}$.

3.5 RLNC Estimation at Eve

Trying to decode the image shared from Alice, Eve however does not know the RLNC coefficients, i.e. α_A and α_S, and the index of the image in the shared datastore, i.e. I_S, which was used at Alice for mixing it with the original image. Therefore, Eve has to estimate the RLNC parameters and select the right image in the datastore to recover the image.

The RLNC coefficients estimated at Eve can be written by

$$\hat{\alpha}_A = \alpha_A \pm \varepsilon_A, \tag{6}$$

$$\hat{\alpha}_S = 1 - \hat{\alpha}_A, \tag{7}$$

where $\hat{\alpha}_A$ and $\hat{\alpha}_S$ are estimated RLNC coefficients of α_A and α_S, respectively, and ε_A denotes the estimation error of α_A at Eve knowing the fact that $\hat{\alpha}_A + \hat{\alpha}_S = 1$.

In addition to the RLNC coefficients, Eve needs to predict the image in the shared datastore that was used for encoding at Alice. Letting $\hat{I}'_S$ denote the predicted image, Eve can decode the image following the same method at Bob in Subsection 3.4.

3.6 VDSR at Bob and Eve

To be able to recover original images from decoded images by RLNC, the VDSR framework, mentioned in (Kim et al., 2016), was implemented. VDSR was, then, trained with a public available IAPR TC-12 Benchmark dataset. We use simiar hyper-parameters described in (Kim et al., 2016). More specific, the training used batches of size 64, 100 epochs. The learning rate is initially 0.1 and decreased by a factor of 10 every 10 epochs. The VDSR was trained with the scaling factor $\delta = 4$.

Then, the decoded images by RLNC decoding at Bob, i.e. $\hat{I}'_B$, and at Eve, i.e. $\hat{I}'_E$, are fed into VDSR model to obtain the upscaled images at Bob and Eve, denoted by $\hat{I}_B$ and $\hat{I}_E$. respectively. The upscaled images at Bob and Eve can be written by

$$\hat{I}_B = VDSR(\hat{I}'_B), \tag{8}$$

$$\hat{I}_E = VDSR(\hat{I}'_E), \tag{9}$$

respectively, where $VDSR(\cdot)$ denotes the operator function to reconstruct the images with the scaling factor δ trained before.

It is worth to mention that other SR methods can be exploited to replace VDSR.

4 EVALUATION METHOD OF THE PROPOSED DEEP NC

In order to evaluate the effectiveness of the proposed Deep-NC for secure VDSR, Peak Signal-to-Noise Ratio (PSNR) is presented in this section as a performance metric to compare the quality of the recovered image at Bob and Eve, i.e. $\hat{I}_B$ and $\hat{I}_E$, with the original HR image transmitted from Alice, i.e. I_A.

The peak signal-to-noise ratio (PSNR) is the ratio between a signal's maximum power and the power of the signal's noise. Engineers commonly use the PSNR to measure the quality of reconstructed images that have been compressed. Each picture element (pixel) has a color value that can change when an image is compressed and then uncompressed. Signals can have a wide dynamic range, so PSNR is usually expressed in decibels, which is a logarithmic scale.

As a well-known image comparison metric, the PSNR is considered to evaluate the loss of the image quality. In the proposed secure ISR, the loss is due to not only the noise at Bob, but also the lack of details in the LR downscaled image and the training loss in the VDSR network.

The PSNR, in dB, of the recovered image $\hat{I}_B$ at Bob with respect to the original image I_A is defined as[4]

$$\text{PSNR} \triangleq 10\log_{10} \frac{1}{\text{MSE}}, \tag{10}$$

where MSE is the mean square error between $\hat{I}_B$ and I_A given by

$$\text{MSE} \triangleq E \left[\left(I_A - \hat{I}_B \right)^2 \right]. \tag{11}$$

Here, $E[\cdot]$ denotes the expectation operator.

Considering RGB colour images having size $M \times N$ with three RGB values per pixel, the MSE can be calculated by

$$\text{MSE} = \frac{1}{3MN} \sum_{x=1}^{M} \sum_{y=1}^{N} \sum_{z=1}^{3} \left(I_A(x,y,z) - \hat{I}_B(x,y,z) \right)^2. \tag{12}$$

Note that the PSNR at Eve is also evaluated using (10). However, the quality of the recovered image is

---

[4]In this work, the image is in double-precision floating-point data type having maximum possible pixel value of 1.

further degraded due to the unknown reference image and the lack of the information of RLNC coefficients which are only shared between Alice and Bob.

5   Simulation Results

In this section, we present the simulation results of the proposed Deep-NC in terms of PSNR. We first compare the performance at Bob with that at Eve when employing either bicubic interpolation or VDSR[5] for converting the received LR images to the original HR images. The impacts of shared image dataset, Gaussian noise, RLNC coefficients and scaling factor on the performance are then sequentially evaluated to show the enhancement of the proposed scheme in securing the private image from the Eve. The results are obtained by simulation in MATLAB. The training is performed on an image dataset of the IAPR TC-12 benchmark with 20,000 still natural images which are available free of charge and without copyright restrictions (Grubinger et al., 2006). In the following experiment, the scaling factor is set as $\delta = 4$, unless otherwise stated. For validation of the proposed scheme, 20 undistorted images of the Image Processing Toolbox in MATLAB are used as shown in Fig. 2 in which the last image is selected as a reference image.

5.1   Impacts of Shared Image Dataset

In order to decode the original image, apart from the RLNC coefficients, the reference image in the datastore is required to be known at the receiver. Considering the scenario when Eve may not know the reference image used at Alice or may use the incorrect image, Fig. 3 plots the PSNR of the proposed scheme as a function of the noise variance, i.e. σ^2, with respect to different shared images at Eve including the 15th, 16th and 20th reference images. Here, the 20th image is used for the RLNC encoding at Alice. Bicubic interpolation and VDSR are employed as typical ISR for upscaling. It can be observed in Fig. 3 that the PSNR at Eve is considerably degraded when the wrong reference image is selected for decoding. For instance, in the noise-free environment with VDSR upscaling, the PSNR at Eve decreases by 7 dB when using the 15th or 16th image instead of the 20th image. A further notice is the fact that, without knowledge of the RLNC coefficient, Eve can only achieve

---

[5]It is worth to notice that the VDSR is selected as a typical ISR to validate the effectiveness of the proposed Deep-NC in securing the image. A comparison of different ISR schemes is beyond the scope of this work.

a close performance to Bob even with the right reference image. This accordingly reflects the effectiveness of the proposed scheme in securing the original image. Furthermore, as shown in Fig. 3, Bob achieves a much better performance than Eve of up to 32 dB when Eve implements only bicubic interpolation. This is due to the fact that no SR is involved in the image processing at Eve in this case along with estimation error of RLNC coefficient and the unknown reference image.

5.2   Impacts of Noise

Considering AWGN model in image communication over wireless medium, Fig. 4 plots the PSNR of the proposed scheme versus noise variance, i.e. σ^2 with the assumption that Bob and Eve experience the same noise model. Two typical upscaling schemes, i.e. the bicubic interpolation and VDSR, are employed at Bob and Eve. The reference image shared to Bob is also leaked to Eve. Intuitively, it can be seen that the PSNR decreases as the noise variance increases. Over the wireless medium, the VDSR is shown to be beneficial providing a higher PSNR than the bicubic interpolation. Similarly, Bob is shown to achieve a better performance than Eve over the whole range of noise variance with both bicubic interpolation and VDSR, though the performance gap is smaller in the more lossy environment. For instance, with the VDSR upscaling, the PSNR at Bob is 3 dB and 2 dB higher than that at Eve, while a considerable enhancement of 14 dB and 13 dB can be achieved with the bicubic interpolation when $\sigma^2 = 0.1$ and $\sigma^2 = 0.2$, respectively.

5.3   Impacts of RLNC coefficients

Investigating the impacts of RLNC coefficients on the performance of the proposed scheme, Fig. 5 plots the PSNR of the proposed scheme versus the RLNC coefficient of the original image, i.e. α_A, with respect to different noise variances at Bob and Eve. Specifically, two noise variances, i.e. $\sigma_B^2 = \sigma_E^2 = \sigma^2 = \{0.1, 0.2\}$, are considered. It can be seen that Bob achieves a better performance than Eve for all RLNC coefficients. Also, the PSNR at both Bob and Eve increases as α_A increases. This is due to the fact that there is more information of the original image in the mixed image. As noted in Remark 1, the RLNC coefficients should be selected so as to restrict Eve from recovering the original image, while maintaining the higher image decodability at Bob. For instance, α_A should be less than 0.5 to limit the PSNR at Eve by 14 dB when $\sigma^2 = 0.1$. The PSNR coefficients should be thus selected depending also on the noise variance.
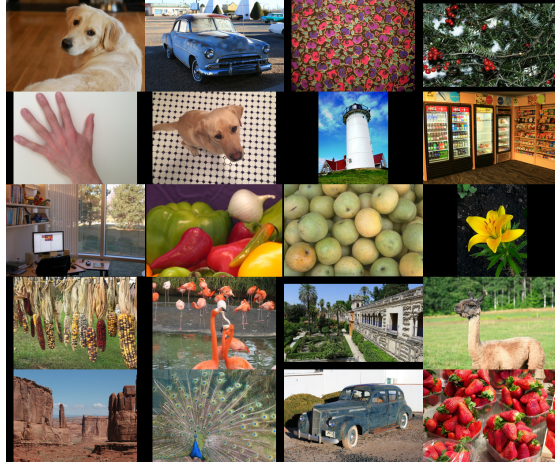
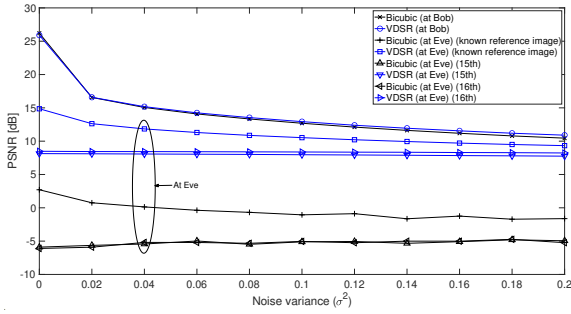Figure 2: Images for evaluation of the proposed Deep-NC.

Figure 3: PSNR versus noise variance with respect to different shared images at Eve.
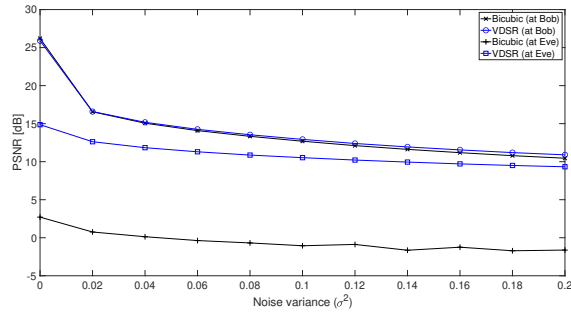

Figure 5: PSNR versus RLNC coefficient of original image.

Figure 4: PSNR versus noise variance in Gaussian white noise model.
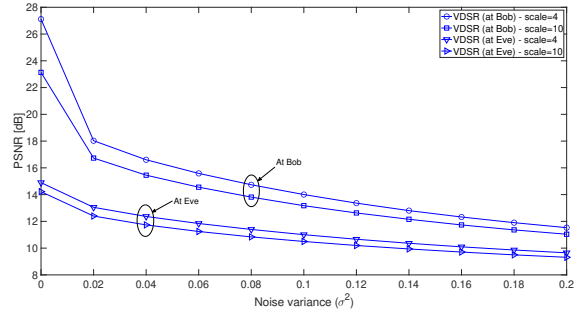
Figure 6: PSNR versus noise variance with respect to different scaling factors.

As shown in Fig. 5, with the same requirement of the maximal PSNR at Eve by 14 dB, α_A should not be greater than 0.5 and 0.7 when $\sigma^2 = 0.1$ and $\sigma^2 = 0.2$, respectively.

5.4 Impacts of Scaling Factor

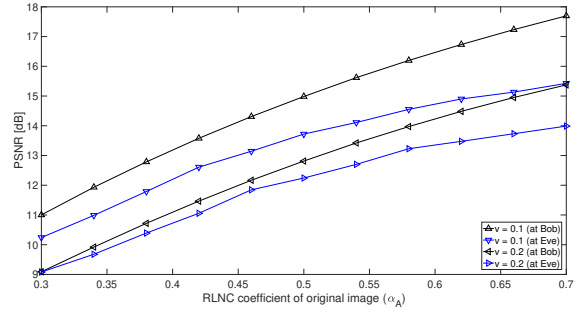The impacts of scaling factor are shown in Fig. 6 where the PSNR at Bob and Eve of the proposed

scheme is plotted against noise variance in AWGN model, i.e. σ^2, with different scaling factors, i.e. $\delta = 4$ and $\delta = 10$. VDSR is considered with the same settings as in Fig. 4. It can be seen in Fig. 6 that the PSNR at Bob decreases considerably in the noiseless environment as the scale increases, while there is not much difference in the PSNR in the noisy environment. For instance, 4 dB is reduced when $\sigma^2 = 0$, while less than 1 dB when $\sigma^2 > 0.1$. This means that

over the noisy medium, the image can be downscaled with a higher scaling factor to save the bandwidth with negligible performance loss.

6 CONCLUSIONS

In this paper, we have proposed a Deep-NC protocol for secure ISR communication between Alice and Bob taking into account Gaussian noise model. Specifically, RLNC has been adopted to protect the secret image from Eve. It has been shown that Bob achieves a much higher PSNR than Eve of up to 32 dB with the proposed Deep-NC protocol. Additionally, an enhanced performance has been shown to achieve at Bob over the whole range of noise variance in Gaussian model. Furthermore, the Deep-NC protocol enables the original image to be downscaled to a much lower resolution prior to transmitting over the lossy environment, which accordingly implies the effectiveness of the proposed scheme in saving the transmission bandwidth.

REFERENCES

Ahlswede, R., Ning Cai, Li, S. . R., and Yeung, R. W. (2000). Network information flow. *IEEE Transactions on Information Theory*, 46(4):1204–1216.

Bender, W., Gruhl, D., Morimoto, N., and Lu, A. (1996). Techniques for data hiding. *IBM Systems Journal*, 35(3.4):313–336.

Chen, P.-Y. and Lin, H.-J. (2006). A DWT based approach for image steganography. *International Journal of Applied Science and Engineering*, pages 275–290.

Duchon, C. E. (1979). Lanczos Filtering in One and Two Dimensions. *Journal of Applied Meteorology*, 18(8):1016–1022.

Franz, E., Jerichow, A., Möller, S., Pfitzmann, A., and Stierand, I. (1996). Computer based steganography: How it works and why therefore any restrictions on cryptography are nonsense, at best. In Anderson, R., editor, *Information Hiding*, pages 7–21, Berlin, Heidelberg. Springer Berlin Heidelberg.

Goodfellow, I., Bengio, Y., and Courville, A. (2016). *Deep learning*. MIT press.

Grubinger, M., Clough, P. D., Müller, H., and Deselaers, T. (2006). The IAPR TC-12 benchmark: A new evaluation resource for visual information systems. https://www.imageclef.org/photodata.

Guerrini, F., Dalai, M., and Leonardi, R. (2020). Minimal information exchange for secure image hash-based geometric transformations estimation. *IEEE Transactions on Information Forensics and Security*, 15:3482–3496.

Haris, M., Shakhnarovich, G., and Ukita, N. (2018). Deep back-projection networks for super-resolution. In *2018 IEEE/CVF Conference on Computer Vision and Pattern Recognition*, pages 1664–1673.

Irani, M. and Peleg, S. (1991). Improving resolution by image registration. *CVGIP: Graphical Models and Image Processing*, 53(3):231 – 239.

Keys, R. (1981). Cubic convolution interpolation for digital image processing. *IEEE Transactions on Acoustics, Speech, and Signal Processing*, 29(6):1153–1160.

Kim, J., Kwon Lee, J., and Mu Lee, K. (2016). Accurate image super-resolution using very deep convolutional networks. In *Proceedings of the IEEE conference on computer vision and pattern recognition*, pages 1646–1654.

Koetter, R. and Medard, M. (2003). An algebraic approach to network coding. *IEEE/ACM Transactions on Networking*, 11(5):782–795.

Lai, W., Huang, J., Ahuja, N., and Yang, M. (2017). Deep laplacian pyramid networks for fast and accurate super-resolution. In *2017 IEEE Conference on Computer Vision and Pattern Recognition (CVPR)*, pages 5835–5843.

Li, Y., Liu, D., Li, H., Li, L., Li, Z., and Wu, F. (2019a). Learning a convolutional neural network for image compact-resolution. *IEEE Transactions on Image Processing*, 28(3):1092–1107.

Li, Z., Yang, J., Liu, Z., Yang, X., Jeon, G., and Wu, W. (2019b). Feedback network for image super-resolution. In *2019 IEEE/CVF Conference on Computer Vision and Pattern Recognition (CVPR)*, pages 3862–3871.

Peng, H., Yang, B., Li, L., and Yang, Y. (2020). Secure and traceable image transmission scheme based on semitensor product compressed sensing in telemedicine system. *IEEE Internet of Things Journal*, 7(3):2432–2451.

Smith, P. (1981). Bilinear interpolation of digital images. *Ultramicroscopy*, 6(1):201 – 204.

Wang, Z., Chen, J., and Hoi, S. C. H. (2020). Deep learning for image super-resolution: A survey. *IEEE Transactions on Pattern Analysis and Machine Intelligence*, pages 1–1.

Xie, X.-Z., Chang, C.-C., and Lin, C.-C. (2019). Reversibility-oriented secret image sharing mechanism with steganography and authentication based on code division multiplexing. *IET Image Processing*, 13(9):1411–1420.

Zhang, K., Zuo, W., Chen, Y., Meng, D., and Zhang, L. (2017). Beyond a Gaussian denoiser: Residual learning of deep CNN for image denoising. *IEEE Transactions on Image Processing*, 26(7):3142–3155.